Biosynthesis and Defensive Function of N^δ-Acetylornithine, a Jasmonate-Induced *Arabidopsis* Metabolite [C][W]

Adewale M. Adio,[a] Clare L. Casteel,[a] Martin De Vos,[a] Jae Hak Kim,[a,1] Vijay Joshi,[a,2] Baohua Li,[b] Caroline Juéry,[a] Josquin Daron,[a] Daniel J. Kliebenstein,[b] and Georg Jander[a,3]

[a] Boyce Thompson Institute for Plant Research, Ithaca, New York 14853

[b] Department of Plant Sciences, University of California, Davis, California 95616

Since research on plant interactions with herbivores and pathogens is often constrained by the analysis of already known compounds, there is a need to identify new defense-related plant metabolites. The uncommon nonprotein amino acid N^δ-acetylornithine was discovered in a targeted search for *Arabidopsis thaliana* metabolites that are strongly induced by the phytohormone methyl jasmonate (MeJA). Stable isotope labeling experiments show that, after MeJA elicitation, Arg, Pro, and Glu are converted to Orn, which is acetylated by NATA1 to produce N^δ-acetylornithine. MeJA-induced N^δ-acetylornithine accumulation occurs in all tested *Arabidopsis* accessions, other *Arabidopsis* species, *Capsella rubella*, and *Boechera stricta*, but not in less closely related Brassicaceae. Both insect feeding and *Pseudomonas syringae* infection increase *NATA1* expression and N^δ-acetylornithine accumulation. *NATA1* transient expression in *Nicotiana tabacum* and the addition of N^δ-acetylornithine to an artificial diet both decrease *Myzus persicae* (green peach aphid) reproduction, suggesting a direct toxic or deterrent effect. However, since broad metabolic changes that are induced by MeJA in wild-type *Arabidopsis* are attenuated in a *nata1* mutant strain, there may also be indirect effects on herbivores and pathogens. In the case of *P. syringae*, growth on a *nata1* mutant is reduced compared with wild-type *Arabidopsis*, but growth in vitro is unaffected by N^δ-acetylornithine addition.

INTRODUCTION

Plants exhibit a wide array of defenses against herbivores and pathogens, ranging from the production of toxins and feeding deterrents (Agrawal, 1998; Kessler and Baldwin, 2002) to compensatory growth changes that allow tolerance of high damage levels (Agrawal, 2000; Stowe et al., 2000; Tiffin, 2000). Many, perhaps most, of the likely several hundred thousand secondary metabolites found in the plant kingdom contribute to defense against herbivores and pathogens (Dixon, 2001; Bino et al., 2004). Broadly distributed classes of secondary metabolites, which can be found as components of both constitutive and inducible plant defense responses, include phenolics, terpenes, alkaloids, and nonprotein amino acids (Howe and Jander, 2008).

In addition to the standard 20 proteinogenic amino acids, hundreds of other amino acids have been found in many different plant species (Fowden, 2001; Bell, 2003). Some of these, for example, Orn and homoserine, are essential in primary metabolism, whereas others are secondary metabolites that contribute

to plant defense against herbivores and pathogens. For instance, canavanine, which is found in the seeds of many legumes, is toxic to herbivores because it competes with Arg in enzymatic reactions (Rosenthal, 2001). Similarly, azetidine-2-carboxylate, which is particularly abundant in *Convallaria majalis* (lily of the valley), can disrupt protein structures by binding to tRNA in place of Pro during protein synthesis (Peterson and Fowden, 1963; Norris and Fowden, 1972).

Another function for nonprotein amino acids may be to store nitrogen in a form that makes it metabolically unavailable to herbivores. About half of the 20 protein amino acids are essential dietary constituents because they cannot be synthesized by most animals. Degradation of Arg to Orn by tomato (*Solanum lycopersicum*) arginase significantly reduces *Manduca sexta* (tobacco hornworm) weight gain (Chen et al., 2005), showing that availability of a single essential amino acid can be growth-limiting for insects. Similarly, conversion of an essential amino acid into an uncommon nonprotein amino acid that herbivores cannot use would reduce the nutritive value of plant tissue.

The nonprotein amino acid N^δ-acetylornithine (Figure 1A) has been reported in *Corydalis ochotensis* (Manske, 1937), *Asplenium nidus* (Virtanen and Linko, 1955), *Bistorta bistortoides* (Lipson et al., 1996), some grasses (Fowden, 1958), and several legumes (Brown and Fowden, 1966; Zacharius, 1970; Kite and Ireland, 2002; Marona et al., 2003). Abundance of N^δ-acetylornithine in legume seeds (Brown and Fowden, 1966; Zacharius, 1970; Kite and Ireland, 2002) and *B. bistortoides* rhizomes (38% of free amino acids; Lipson et al., 1996) suggests a role in nitrogen storage. However, given that N^δ-acetylornithine has
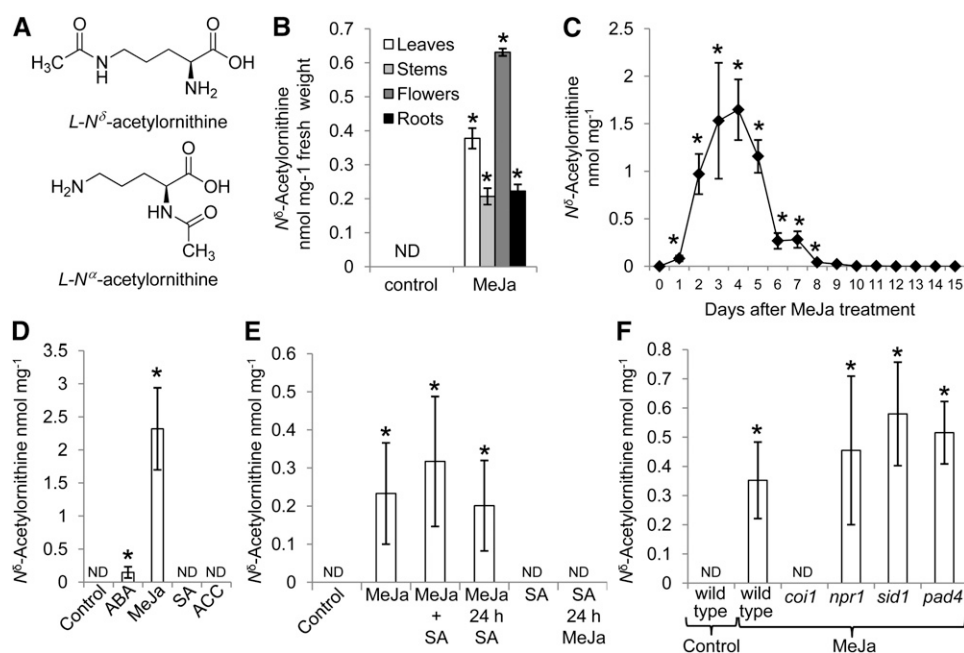
Figure 1. Regulation of N^δ-Acetylornithine Production in *Arabidopsis*.

(A) Structures of L-N^δ-acetylornithine and L-N^α-acetylornithine.

(B) Accumulation of N^δ-acetylornithine in plant tissues 4 d after MeJA treatment. Mean ± SE of n = 3. ND, not detected.

(C) Time course of N^δ-acetylornithine accumulation in rosette leaves after MeJA treatment. Mean ± SE of n = 3.

(D) N^δ-acetylornithine accumulation 4 d after spraying with 450 μM MeJA, SA, ACC, or 100 μM ABA. Mean ± SE of n = 3.

(E) Inhibition of N^δ-acetylornithine biosynthesis by SA. SA was added 24 h before, concomitant with MeJA, or 24 h later. N^δ-acetylornithine in rosette leaves was measured 4 d after the treatment. Mean ± SE of n = 5.

(F) N^δ-acetylornithine in *Arabidopsis* defense signaling mutants, 4 d after MeJA treatment. Mean ± SE of n = 4 or 5. *P < 0.05, t test relative to unelicited control plants or day 0 time point **(C)**.

been found sporadically in ferns, monocots, and dicots (in the Aspleniaceae, Fabaceae, Papaveraceae, Poaceae, and Polygonaceae), there may be additional functions associated with this plant metabolite. Like most nonprotein amino acids found in plants, N^δ-acetylornithine has not been studied in a genetically tractable model species and almost nothing is known about the biosynthetic pathway(s).

Research with *Arabidopsis thaliana* has identified diverse classes of secondary metabolites (D'Auria and Gershenzon, 2005), and, in particular, the defense-related glucosinolates have been studied extensively (Halkier and Gershenzon, 2006). However, very little is known about defensive nonprotein amino acids in *Arabidopsis*, and the majority of the estimated 5000 small molecules in a typical leaf remain unidentified (Bino et al., 2004). The plant hormone jasmonic acid (JA) and its more volatile form, methyl jasmonate (MeJA), induce numerous defense responses, including production of secondary metabolites, in *Arabidopsis* and other plants (Howe and Jander, 2008). Therefore, in an effort to identify and study previously unknown plant chemical defenses, we initiated a search for the MeJA-induced production of nonprotein amino acids in *Arabidopsis*. These experiments resulted in the identification of N^δ-acetylornithine, an Orn acetyltransferase that synthesizes this compound and likely defensive functions.

RESULTS

Induced Production of N^δ-Acetylornithine in *Arabidopsis*

Assays of phloem exudates from MeJA-induced *Arabidopsis* accession Columbia-0 (Col-0) showed accumulation of an unknown amino acid, which was determined to be N^δ-acetylornithine (Figure 1A) by mass spectrometry (MS) and NMR (see Supplemental Figure 1 online). N^δ-acetylornithine, which was not commercially available, was synthesized and shown to have the same properties as the purified *Arabidopsis* compound (see Supplemental Figures 1 and 2 online). The absolute configuration of *Arabidopsis* N^δ-acetylornithine was determined to be *L* by comparing the polarity of the purified *Arabidopsis* metabolite to synthesized L-N^δ-acetylornithine and a racemic D-L mixture. N^δ-acetylornithine, which has not been previously reported in *Arabidopsis* or other Brassicaceae, is distinct from N^α-acetylornithine (Figure 1A; see Supplemental Figure 2 online), an intermediate in plant Arg and Pro metabolism that is found in most, perhaps all, plants (Verslues and Sharma, 2010).

After treatment of with MeJA, N^δ-acetylornithine was detected in *Arabidopsis* leaves, stems, flowers, and roots (Figure 1B). Accumulation in rosette leaves peaked after 4 d and returned to undetectable levels by day 10 (Figure 1C), suggesting that there

is also an N^δ-acetylornithine catabolic pathway in *Arabidopsis*. Other defense-related plant hormones were tested to determine whether they induce N^δ-acetylornithine accumulation. N^δ-acetylornithine abundance in leaves increased with increasing concentrations of exogenously added abscisic acid (ABA) (Figure 1D; see Supplemental Figure 3 online). By contrast, there was no detectable N^δ-acetylornithine after treatment with salicylic acid (SA) or the ethylene precursor 1-aminocyclopropane-1-carboxylate (ACC). SA inhibited the MeJA-induced production of N^δ-acetylornithine (Figure 1E), albeit only if it was applied 24 h before the MeJA. This is consistent with several prior studies showing antagonistic effects in plant defense induction and reduced effectiveness of MeJA elicitation once SA-mediated defenses are turned on (Thaler et al., 2002; Spoel et al., 2003; Mur et al., 2006). The *nonexpresser of pr genes1* (*npr1*), *salicylic acid induction deficient1* (*sid1*), and *phytoalexin deficient4* (*pad4*) mutations, which result in defects in SA-related defense signaling, had no significant effect on N^δ-acetylornithine induction by MeJA (Figure 1F). Furthermore, these mutants did not have any detectable N^δ-acetylornithine in the absence of MeJA elicitation. By contrast, there was no MeJA-induced N^δ-acetylornithine accumulation in the *coronatine insensitive1-1* (*coi1-1*) mutant (Figure 1F), indicating that induction requires a functional COI1 receptor, similar to most other JA-mediated responses in *Arabidopsis* (Chini et al., 2007; Thines et al., 2007).

Biosynthesis of N^δ-Acetylornithine from Other Amino Acids

The structure of N^δ-acetylornithine suggested that it could be synthesized from Arg, Glu, or Pro, with Orn as an intermediate (Figure 2A; other pathways are also possible). If so, addition of [U-^{13}C]Arg, [U-^{13}C]Pro, or [U-^{13}C]Glu to *Arabidopsis* leaves should result in the synthesis of [^{13}C]N^δ-acetylornithine with a mass of +5 atomic mass units (see Supplemental Figure 4 online). As predicted, gas chromatography (GC)-MS analysis of N^δ-acetylornithine in MeJA-treated plants after the addition of ^{13}C-labeled precursor amino acids showed significant incorporation from Arg, Pro, and Glu (Figure 2B). Although the labeling results showed a direct conversion of the three amino acids into N^δ-acetylornithine, the multiple pathways leading to Orn formation (Figure 2A) suggested that knockout of any one amino acid catabolic enzyme would not significantly reduce N^δ-acetylornithine accumulation. Consistent with this hypothesis, knockout mutations in either of the two *Arabidopsis* arginases (*ARGININE AMINOHYDROLYASE1* [*ARGAH1*] and *ARGAH2*; Brownfield et al., 2008) did not decrease N^δ-acetylornithine abundance (Figure 2C). In fact, for as yet unknown reasons, the *argah2* mutation increased MeJA-induced N^δ-acetylornithine levels.

Orn Acetyltransferase Mutant Isolation and Characterization

Given the incorporation of five carbon atoms from Arg, Pro, and Glu into N^δ-acetylornithine, we hypothesized that there is an Orn N^δ-acetyltransferase in *Arabidopsis* that converts Orn into N^δ-acetylornithine (Figure 2A). Analysis of publications reporting MeJA-regulated *Arabidopsis* gene expression showed elevated transcription of At2g39030, a member of the GNAT (Gcn5-related *N*-acetyltransferase) family of acetyltransferases (Vetting et al., 2005; Yan et al., 2007). Publicly available DNA microarray data also showed that At2g39030 is induced by JA,
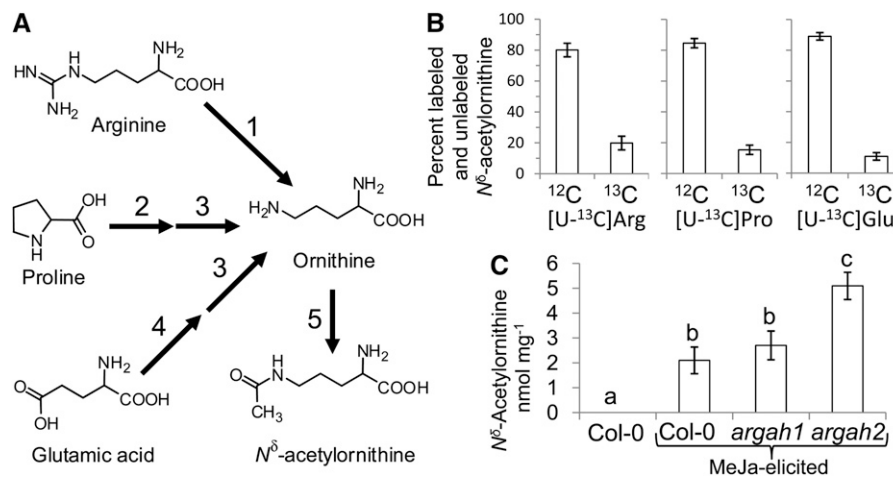
Figure 2. Biosynthesis of N^δ-Acetylornithine from Other Amino Acids.

(A) Possible pathways leading from Arg, Pro, and Glu to N^δ-acetylornithine. 1, Arginase (At2g39020 and At4g08900); 2, Pro dehydrogenase (At3g30775 and At5g38710); 3, Orn δ-aminotransferase (At5g46180); 4, pyrroline-5-carboxylate synthase (At2g39800 and At3g55610); 5, Orn N^δ-acetyltransferase (At2g39030).

(B) Incorporation of [U-^{13}C]Arg, [U-^{13}C]Pro, and [U-^{13}C]Glu into N^δ-acetylornithine in MeJA-treated *Arabidopsis* leaves, expressed as the percentage of labeled [^{13}C$_5$]N^δ-acetylornithine and unlabeled [^{12}C]N^δ-acetylornithine in rosette leaves. Mean ± SE of n = 3.

(C) N^δ-acetylornithine accumulation in arginase mutants. Mean ± SE of n = 5. Letters indicate significant differences, P < 0.05, analysis of variance, followed by Tukey's HSD test.

ABA, mechanical wounding, and a variety of biotic stresses, including *Myzus persicae* (green peach aphid) and *Pseudomonas syringae* (www.genevestigator.com; Zimmermann et al., 2004).

To determine whether At2g39030 encodes an Orn N^6-acetyltransferase, we obtained the only available knockout line (GK-256F07; Rosso et al., 2003). Presence of a homozygous T-DNA insertion and lack of mRNA was confirmed by PCR and quantitative real-time RT-PCR (qRT-PCR), respectively. The mutant had no obvious visible defects and initiated flowering at the same time as wild-type Col-0. However, in contrast with the wild-type controls, no N^6-acetylornithine was found in GK-256F07 leaves (Figure 3A), stems, flowers, and roots after MeJA treatment, indicating that At2g39030 encodes an Orn N^6-acetyltransferase. We named the At2g39030 gene *NATA1* (for *N*-Acetyltransferase Activity1) and the GK-256F07 mutant allele *nata1-1*. At2g39020, a gene that is directly adjacent to *NATA1* in the Col-0 genome, encodes a predicted protein that is 78% identical to NATA1 at the amino acid sequence level and is also annotated as a putative GNAT. Amino acid analysis of the only available At2g39020 T-DNA insertion line (Salk_092319; Alonso et al., 2003) showed no change in the MeJA-induced accumulation of N^6-acetylornithine (Figure 3A).

The function of *NATA1* in N^6-acetylornithine biosynthesis was confirmed by complementing the *nata1-1* mutation with a *35S:NATA1* construct, which caused constitutive production of N^6-acetylornithine (Figure 3B). Although *NATA1* overexpression decreased Orn and Pro levels and increased some other amino acids (see Supplemental Figure 5 online), there was no significant difference in the total free amino acid content between wild-type Col-0 and the *35S:NATA1* line. N^6-acetylornithine also accumulated after transient *NATA1* expression in *Nicotiana benthamiana*, which does not normally produce this amino acid (Figure 3C). By contrast, At2g39020 transient expression in *N. benthamiana* caused no detectable

N^6-acetylornithine accumulation. Together, these results confirmed that NATA1 functions in the biosynthesis of N^6-acetylornithine in *Arabidopsis*.

NATA1 expression was induced by MeJA, with a significant, 20-fold increase observed within 1.5 h after treatment (Figure 3D) and a peak in transcript abundance after 24 h. Relative gene expression after 24 h in this experiment was quite high due to the very low, almost undetectable expression of *NATA1* at the zero-hour time point. Over a period of several days after MeJA treatment, *NATA1* expression declined back to basal levels. This gene expression pattern was consistent with the observed changes in N^6-acetylornithine accumulation after MeJA treatment (Figure 1C), but with the increase in gene expression preceding metabolite accumulation.

P. syringae Induces N^6-Acetylornithine Accumulation

The requirement of a functional *COI1* gene for N^6-acetylornithine accumulation (Figure 1F) suggested that infection with *P. syringae*, which produces the JA-Ile mimic coronatine, should also induce N^6-acetylornithine production. Coronatine itself induced N^6-acetylornithine accumulation in a concentration-dependent manner (Figure 4A). Spray inoculation with two virulent bacterial isolates, *P. syringae* pv *tomato* DC3000 (DC3000) and *P. syringae* pv *maculicola* 4326 (Psm4326), also induced N^6-acetylornithine production (Figure 4A). However, there was much lower N^6-acetylornithine accumulation after similar inoculation with coronatine-deficient *P. syringae* mutants (Brooks et al., 2004; Cui et al., 2005). Since coronatine inhibits stomatal closure, thereby facilitating successful *P. syringae* infection (Melotto et al., 2006), these experiments were done under high humidity conditions, which promote stomatal opening and allow similar entry and growth of coronatine mutant and wild-type *P. syringae*. In the *flagellin-sensitive2* (*fls2*) mutant background, where the stomatal closure response to *P. syringae* is compromised and coronatine
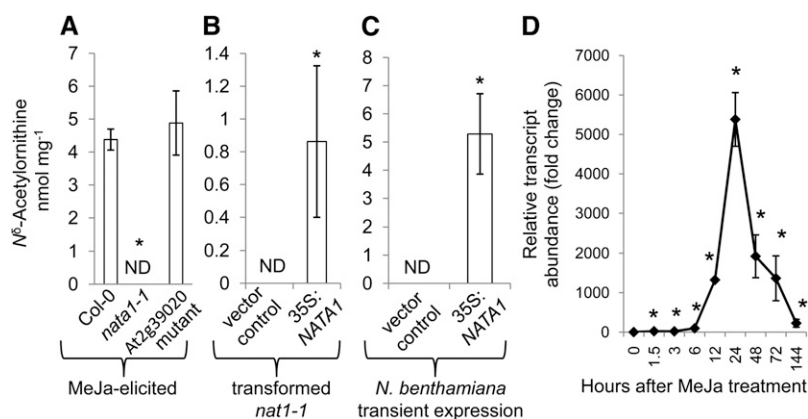

Figure 3. N^6-Acetylornithine Biosynthesis Requires NATA1 (At2g39030).

(A) N^6-acetylornithine biosynthesis in *nata1-1* and an At2g39020 T-DNA insertion mutant, 4 d after MeJA treatment. Mean ± SE of *n* = 5. ND, not detected.
(B) Expression of p35S:*NATA1* causes constitutive N^6-acetylornithine production in *nata1-1*. Mean ± SE of *n* = 3.
(C) p35S:*NATA1* transient expression in *N. benthamiana* results in N^6-acetylornithine production. Mean ± SE of *n* = 5.
(D) *NATA1* expression over time after MeJA treatment of wild-type Col-0. Mean ± SE of *n* = 3 to 9. *P < 0.05, *t* test relative to control or 0 h time point.
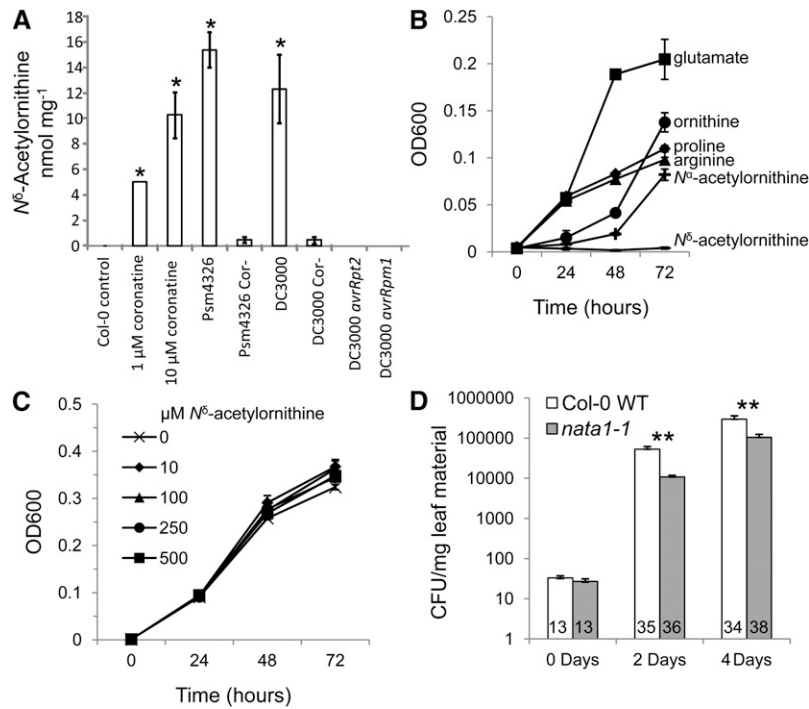
Figure 4. N^δ-Acetylornithine Effects on *P. syringae*.

(A) N^δ-acetylornithine accumulation in wild-type Col-0 4 d after treatment with coronatine, coronatine-producing and nonproducing (Cor-) *P. syringae* strains Psm4326 and DC3000, and DC3000 carrying the avirulence genes *avrRpt2* and *avrRpm1*. Mean $\pm$ SE of $n = 5$, *$P < 0.05$, t test relative to control.
(B) Growth of *P. syringae* DC3000 in minimal maltose medium with 2 g L^{-1} of a single amino acid as the nitrogen source. Mean $\pm$ SE of $n = 3$.
(C) Growth of *P. syringae* in minimal maltose medium with 0, 10, 100, 250, or 500 μM N^δ-acetylornithine and 2 g L^{-1} Glu as the nitrogen source. Mean $\pm$ SE of $n = 3$.
(D) Growth of *P. syringae* DC3000 infiltrated into Col-0 wild-type and *nata1-1* mutant leaves. CFU, colony-forming units. Numbers in bars indicate sample sizes $\pm$ SE. **$P < 0.01$, t test.

is not required for entry (Zeng and He, 2010), there was also reduced N^δ-acetylornithine induction by coronatine-mutant *P. syringae* (see Supplemental Figure 6 online). Inoculation of wild-type Col-0 with DC3000 *avrRpt2* (Whalen et al., 1991) and DC3000 *avrRpm1* (Century et al., 1995) did not cause N^δ-acetylornithine accumulation (Figure 4A). Two possible explanations for this lack of induction are enhanced *Arabidopsis* SA production in response to avirulent *P. syringae* and reduced coronatine production due to the slower growth of these strains.

P. syringae strain DC3000 was able to grow on minimal-maltose medium with Glu, Orn, Pro, Arg, or N^α-acetylornithine as the only nitrogen source (Figure 4B). However, there was no significant growth with N^δ-acetylornithine, showing that this amino acid cannot be used as a nitrogen source by *P. syringae*. When N^δ-acetylornithine was added to minimal medium containing Glu as a nitrogen source, there was no *P. syringae* growth inhibition (Figure 4C), indicating that N^δ-acetylornithine is not toxic or inhibitory. Further experiments were conducted in vivo to determine whether NATA1 activity affected bacterial growth in *Arabidopsis*. Compared with wild-type Col-0, *P. syringae* DC3000 grew significantly less well on *nata-1* mutant plants (Figure 4D), suggesting that induction of *NATA1* expression and N^δ-acetylornithine production by coronatine (Figure 4A) contributed to a successful bacterial infection.

Phloem Localization of N^δ-Acetylornithine

Previous research, including creation of a transgenic *Arabidopsis* line carrying a *NATA1* promoter β-glucuronidase fusion, showed that this gene is expressed predominantly, though not exclusively, in phloem-associated tissue (Wenzel et al., 2008). On a weight-normalized basis, the *NATA1* transcript was more abundant in the midveins of MeJA-treated plants than in the leaf blades ($P < 0.05$, t test; Figure 5A). N^δ-acetylornithine was also abundant in phloem exudates collected from MeJA-treated *Arabidopsis* rosettes (Figure 5B), where it constituted 12% of the free amino acids released from cut stems. Since aphid stylectomy experiments showed 49 mM total amino acid content in *Arabidopsis* phloem (Zhu et al., 2005), we estimated that there is 5.9 mM N^δ-acetylornithine in the phloem sap after MeJA elicitation. This concentration of N^δ-acetylornithine was higher than what we observed in assays of whole leaves and other *Arabidopsis* tissue (Figures 1B to 1F). MeJA elicitation in this experiment also caused a 24% decrease in exudation of the main phloem transport amino acids (Asn, Asp, Gln, and Glu; $P < 0.01$, t test; see Supplemental Figure 7 online), which together constitute ~70% of the total free amino acids in *Arabidopsis* phloem sap (Zhu et al., 2005).
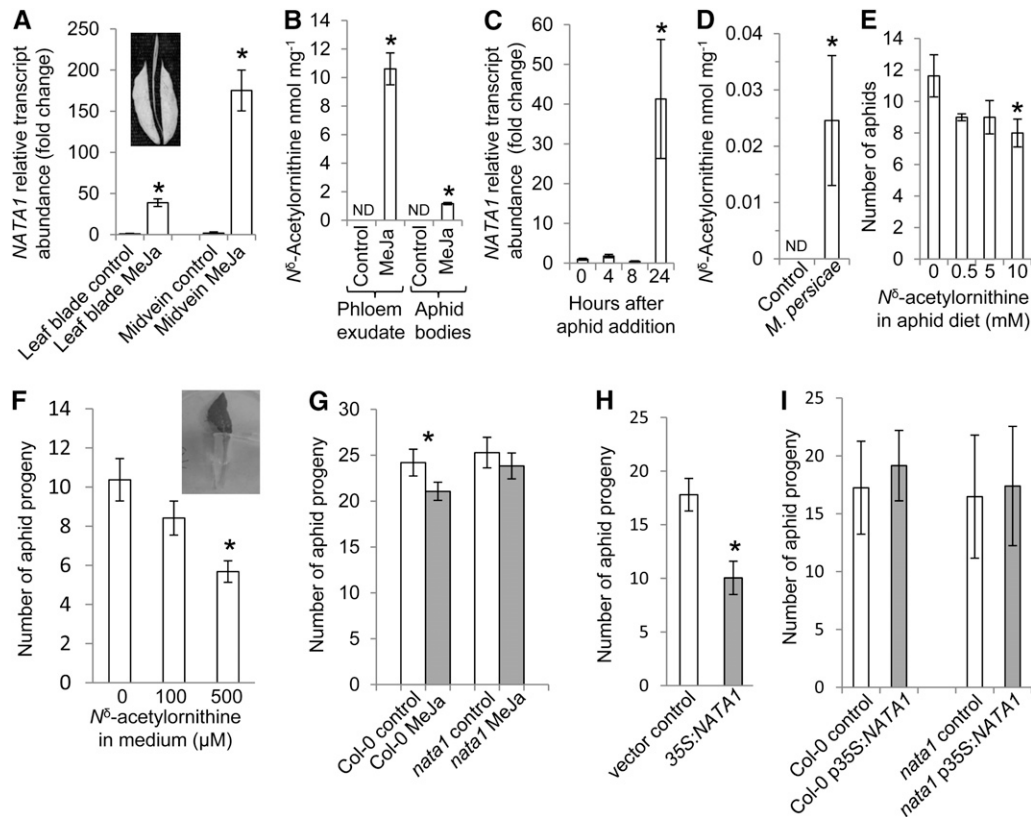
Figure 5. *NATA1* Expression and N^δ-Acetylornithine Affect *Arabidopsis*–*M. persicae* Interactions.

(A) Expression of *NATA1* in dissected leaf blades and midveins (inset), with and without 24 h MeJA elicitation. Mean ± SE of n = 4 or 5.

(B) N^δ-acetylornithine in petiole exudates and aphids feeding for 1 d from plants treated 4 d earlier with MeJA. Mean ± SE of n = 3.

(C) *NATA1* expression with 25 aphids feeding on one leaf. Fold induction, with 0 h set to 1. Mean ± SE of n = 3 or 4.

(D) N^δ-acetylornithine accumulation in Col-0 wild type after 4 d of *M. persicae* feeding. Mean ± SE of n = 3.

(E) Aphid reproduction on artificial diet containing 0 (control), 0.5, 5, or 10 mM N^δ-acetylornithine. Mean ± SE of n = 8.

(F) *M. persicae* reproduction on detached *nata1-1* leaves with petioles in a tube containing N^δ-acetylornithine (see inset). Number of aphid progeny after 4 d. Mean ± SE of n = 22.

(G) *M. persicae* reproduction wild type and *nata1-1* after MeJA treatment. Mean ± SE of n = 19.

(H) *M. persicae* reproduction on *N. tabacum* transiently expressing p35S:*NATA1*. Number of aphid progeny after 7 d. Mean ± SE of n = 25.

(I) *M. persicae* reproduction on *Arabidopsis* wild-type Col-0 and *nata1* mutant transformed with p35S:*NATA1*. Number of aphid progeny after 7 d. Mean ± SE of n = 25 to 27. ND, not detected. *P < 0.05, t test relative to control samples.

N^δ-Acetylornithine Effects on Insect Herbivory

Given the abundance of N^δ-acetylornithine in *Arabidopsis* phloem exudates (Figure 5B), we predicted that this amino acid would also be ingested by phloem-feeding *M. persicae*. This was confirmed through amino acid analysis of whole aphids, which contained N^δ-acetylornithine after short-term (24 h) feeding from MeJA-induced Col-0 but not after feeding from uninduced plants (Figure 5B). Longer infestation with *M. persicae* induced both *NATA1* gene expression (Figure 5C) and N^δ-acetylornithine accumulation (Figure 5D).

To determine whether there was a direct toxic or deterrent effect on *M. persicae*, we added N^δ-acetylornithine to an artificial diet that also contained the 20 protein amino acids. This caused a significant reduction in *M. persicae* progeny production (Figure 5E) at N^δ-acetylornithine concentrations that are comparable to

those that we have observed in phloem exudates. Similarly, exogenous addition of N^δ-acetylornithine to *nata1-1* leaves via their petioles (Figure 5F) significantly reduced aphid reproduction. However, in this detached-leaf experiment, N^δ-acetylornithine addition may also affect aphid reproduction through the reduced abundance of three amino acids (Gly, Arg, and Thr) in the treated leaves relative to controls (see Supplemental Figure 8 online). As a percentage of total amino acid content, N^δ-acetylornithine was 5.9-fold more abundant in the honeydew of *M. persicae* than in the artificial diet from which they were feeding (0.5 mM N^δ-acetylornithine = 0.29% of total amino acids in the artificial diet; 1.7% ± 0.3% N^δ-acetylornithine in the honeydew; mean ± SE of n = 3; P < 0.05, t test). This indicated that N^δ-acetylornithine was taken up and/or metabolized less efficiently than the 20 protein amino acids the aphid diet. Consistent with this observation, addition of Orn or Gln, but not N^δ-acetylornithine, as

the only nitrogen source in artificial diet increased aphid progeny production relative to a Suc-only control diet (see Supplemental Figure 9 online).

Prior work showed that MeJA treatment significantly decreases *M. persicae* reproduction on *Arabidopsis* (Ellis et al., 2002). This effect was confirmed with our *M. persicae* strain on flower stalks of wild-type Col-0 (Figure 5G). However, on *nata1-1* mutant plants, there was no significant reduction in *M. persicae* reproduction due to MeJA treatment, which suggested that *NATA1* plays a role in defense against aphids. Transient expression of *NATA1* from the 35S promoter in tobacco (*Nicotiana tabacum*) caused N^δ-acetyl-ornithine accumulation and decreased *M. persicae* progeny production relative to vector-only controls (Figure 5H). However, stable transgenic expression of the same construct in wild-type Col-0 or *nata1-1* mutant *Arabidopsis* did not have a measureable effect (Figure 5I). Since N^δ-acetylornithine inhibition of *M. persicae* reproduction was concentration dependent (Figures 5E and 5F), this difference may have resulted from lower accumulation of N^δ-acetylornithine in p35S:*NATA1 Arabidopsis* than in transiently expressing p35S:*NATA1 N. tabacum* or MeJA-elicited *Arabidopsis* (Figure 3).

Feeding by two lepidopteran herbivores, *Pieris rapae* (white cabbage butterfly) and *Plutella xylostella* (diamondback moth), induced *NATA1* transcription (Figure 6A) and N^δ-acetylornithine accumulation (Figure 6B). However, the *nata1-1* mutation did not affect *P. rapae* (Figure 6C) or *P. xylostella* (Figure 6D) caterpillar growth.

Metabolic Changes Associated with the *nata1-1* Mutation

Since glucosinolates have been implicated in *Arabidopsis* defense against both *P. syringae* and *M. persicae* (Bednarek et al., 2005; Kim and Jander, 2007; Clay et al., 2009; De Vos and Jander, 2009; Pfalz et al., 2009; Fan et al., 2011), we hypothesized that the *nata1-1* mutation might alter glucosinolate accumulation. However, basal glucosinolate abundance was not

changed in *nata1-1* compared with wild-type Col-0 (see Supplemental Figure 10 online). Similar glucosinolate increases were also observed in *nata1-1* and Col-0 after MeJA treatment, which indicated that the mutant is not compromised in this component of the *Arabidopsis* defense response.

To identify other metabolic changes associated with *NATA1* gene expression, we conducted GC-MS metabolite profiling of wild-type Col-0 and *nata1-1*, with and without MeJA treatment. Our assay detected 290 *Arabidopsis* metabolites, 73 of which were identified based on molecular standards (see Supplemental Data Set 1 online). In the absence of MeJA treatment, the metabolite abundance in Col-0 and *nata1-1* was similar (Figure 7A; see Supplemental Data Set 1 online), as would be expected from the very low basal *NATA1* expression (Figure 3D). Treating wild-type Col-0 with MeJA decreased the abundance of 133 metabolites, including free amino acids, sugars, and tricarbox-ylic acid cycle intermediates (triangles in Figure 7B; see Supplemental Data Set 1 online). There were 24 MeJA-induced metabolites detected in the MS assay (circles in Figure 7B), none of which had a known identity. By contrast, fewer metab-olites were significantly altered (35 induced and 32 repressed; $P < 0.01$, t test) by MeJA treatment of the *nata1-1* mutant (Figure 7C; see Supplemental Data Set 1 online). Agmatine, putrescine, and spermidine were induced by MeJA in the *nata1-1* mutant but not in wild-type Col-0 (see Supplemental Figure 11 online). Most other metabolites that were altered by MeJA in Col-0 were affected to a lesser extent in *nata1-1* (Figure 7D; see Supple-mental Data Set 1 online). For instance, free Phe was reduced by 90% in Col-0 and 50% in *nata1-1*, and free Gln was reduced by 98% in Col-0 and 80% in *nata1-1* by MeJA treatment. Since free amino acids as a source of nitrogen are of particular importance to aphid feeding (Wilson et al., 2010), these were measured in an independent assay (HPLC fluorescence detection) and were found to be significantly less repressed by MeJA in the *nata1-1* mutant than in wild-type Col-0 (see Supplemental Figure 12 online). Although MeJA-induced metabolite changes were attenuated in
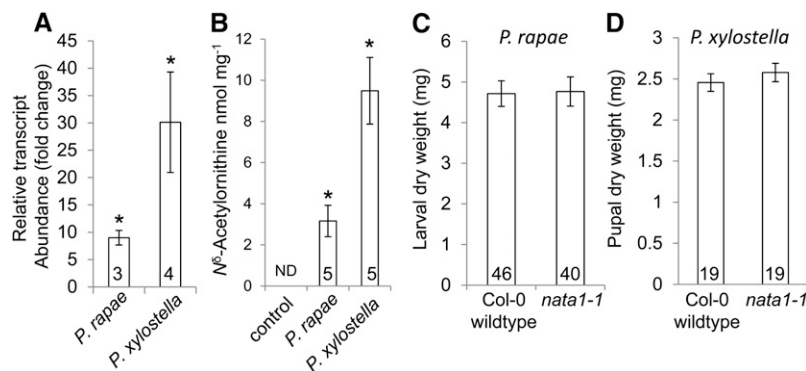

Figure 6. *NATA1* Effects on *P. rapae* and *P. xylostella* Growth.

(A) *NATA1* gene expression 3 d after one neonate caterpillar was placed on a 3-week-old *Arabidopsis* plant. Gene expression on control plants without caterpillars was set to 1.
(B) N^δ-acetylornithine accumulation 7 d after one neonate caterpillar was placed on a 3-week-old *Arabidopsis* plant.
(C) *P. rapae* dry weight 7 d after neonate larvae were placed on wild-type Col-0 or *nata1-1*.
(D) Pupal weight of *P. xylostella* that spent their entire larval growth on Col-0 or *nata1-1*. P values calculated with t tests. *P < 0.05, t test relative to controls. Numbers in bars indicate sample sizes ± SE. ND, not detected.
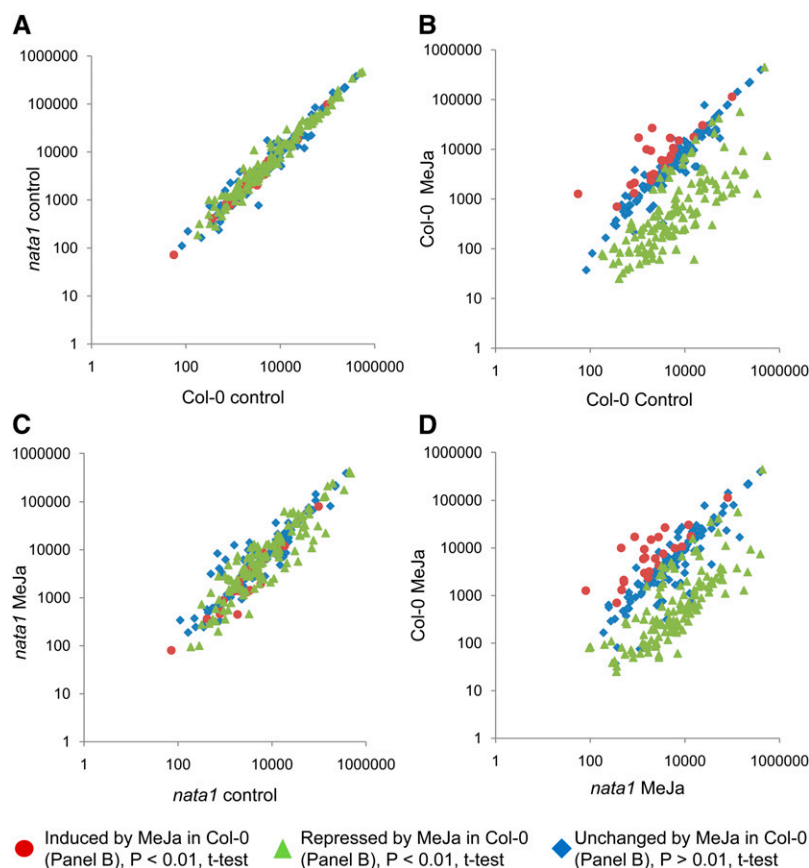
Figure 7. Metabolite Changes Induced 4 d after MeJA Treatment of Wild-Type Col-0 and *nata1-1* Mutant Plants.

(A) Comparison of metabolites in Col-0 and *nata1-1* in the absence of MeJA treatment.
(B) Comparison of metabolites in Col-0 with and without MeJA treatment.
(C) Comparison of metabolites in *nata1-1* with and without MeJA treatment.
(D) Comparison of MeJA-induced metabolites in Col-0 and *nata1-1*. Each data point represents the average of eight independent measurements. *x* and *y* axis units are arbitrary (mass spectrometer counts). Symbols represent the same group of metabolites in each figure, indicating those that are unaltered (diamonds), significantly induced (circles), or significantly repressed (triangles) by MeJA treatment of wild-type Col-0 in **(B)**.
[See online article for color version of this figure.]

the *nata1-1* mutant, plant growth inhibition by MeJA was similar in *nata1-1* and Col-0 (see Supplemental Figure 13 online), indicating that inhibition of primary metabolism can be separated from the growth-inhibitory effects of MeJA.

N^δ-Acetylornithine in Other Plant Species

Amino acid analysis of 25 *Arabidopsis* accessions (see Supplemental Table 1 online) showed MeJA-induced production of N^δ-acetylornithine in every case. We also found MeJA-induced N^δ-acetylornithine accumulation in two other *Arabidopsis* species, as well as in *Capsella rubella* and *Boechera stricta* (Figure 8A). No N^δ-acetylornithine production was found in other tested Brassicaceae: *Barbarea vulgaris*, *Brassica oleracea*, *Brassica rapa*, *Camelina sativa*, *Crucihimalaya lasiocarpa*, *Olimarabidopsis pumila*, *Sisymbrium irio*, *Thellungiella parvula*, and *Thellungiella salsuginea* (see Supplemental Table 2 online). Analysis of publicly available sequence data (see Supplemen-

tal Data Set 2 online) and construction of a phylogenetic tree based on the predicted protein sequences showed likely At2g39020 homologs in several other Brassicaceae, but NATA1 homologs were found only in the genomes of *C. rubella* and *Arabidopsis lyrata* (Figure 8B). As in *Arabidopsis*, the NATA1 and At2g39020 homologs in the *C. rubella* and *A. lyrata* genomes were found to be tandem duplications, with the two genes ~80% identical in their predicted amino acid sequences.

Although N^δ-acetylornithine has been reported in some grasses (Fowden, 1958), we were unable to detect it in *Zea mays*, *Oryza sativa*, *Brachypodium distachion*, and *Setaria viridis*. Tested solanaceous species (*Solanum tuberosum*, *Solanum lycopersicum*, *N. tabacum*, and *N. benthamiana*) did not produce N^δ-acetylornithine, with or without MeJA treatment. Consistent with reports of N^δ-acetylornithine in the seeds of other legume species (Brown and Fowden, 1966; Zacharius, 1970; Kite and Ireland, 2002), *Medicago truncatula* cv Jemalong had 0.035 ± 0.003 nmol/gram N^δ-acetylornithine in the seeds. There was no
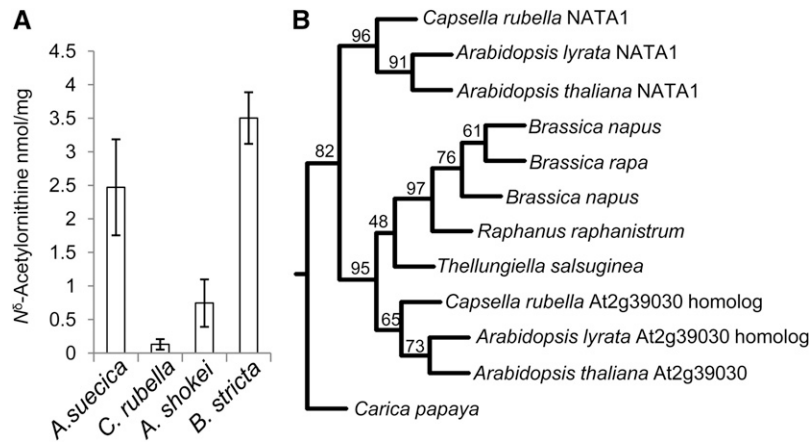
Figure 8. Presence of N^6-Acetylornithine and NATA1-Like Proteins in the Brassicaceae.

(A) N^6-acetylornithine accumulation after MeJA treatment of crucifer species closely related to *Arabidopsis*. Mean ± SE of $n = 3$.

(B) Consensus phylogenetic tree of Brassicaceae NATA1 homologs produced with 1000 replicates. *Carica papaya* (Caricaceae) was used as an outgroup. Values at the branch points indicate bootstrap percentages. The alignment used to generate this tree is available as Supplemental Data Set 2 online.

detectable N^6-acetylornithine in the leaves of this *M. truncatula* accession, with or without MeJA treatment.

DISCUSSION

By finding N^6-acetylornithine and an acetyltransferase (NATA1, At2g39030) that synthesizes this nonprotein amino acid in *Arabidopsis*, we identified a new MeJA-inducible defense response. NATA1 likely contributes in more than one way to the induced *M. persicae* resistance that we and others have observed. Our experiments with N^6-acetylornithine added to aphid artificial diet (Figure 5E) and *Arabidopsis* leaves (Figure 5F) suggest a direct toxic or deterrent effect. However, NATA1 likely also enhances aphid resistance by converting essential phloem amino acids into a form that the insects cannot utilize.

Different resource utilization by aphids, caterpillars, and *P. syringae* may account for the differential effects of the *nata1-1* mutation on these organisms. Whereas aphids depend on nutrients from phloem sap, which contains nitrogen mostly in the form of free amino acids, caterpillars and *P. syringae* benefit from the much more abundant protein-bound amino acids and other forms of nitrogen in whole plant tissue. *Arabidopsis* foliage has 70 mg nitrogen/g dry weight (Lemaître et al., 2008), but only ~2% (1.5 mg nitrogen/g dry weight) is in the form of free amino acids (Lam et al., 2003; Lemaître et al., 2008). Therefore, changes in the abundance of free amino acids, such as those observed due to the *nata1-1* mutation (see Supplemental Figure 12 online), would be have a bigger effect on aphids than on caterpillars and *P. syringae*.

Metabolic differences between aphids and caterpillars may also influence the effects of N^6-acetylornithine on insect herbivory. Insects lack Orn transcarbamylase (Figure 9) and are unable to synthesize Arg from Orn (Reddy and Campbell, 1977; Adams et al., 2000; Honeybee Genome Sequencing Consortium, 2006;

Richards et al., 2008). If plant arginase already makes Arg unavailable for insects (Chen et al., 2005), then subsequent conversion of Orn to N^6-acetylornithine might not provide any additional defensive benefit. Although aphids lack all of the enzymes of the urea cycle (Figure 9; Wilson et al., 2010), they have obligate endosymbiotic bacteria in the genus *Buchnera* that can produce Arg from Orn (Shigenobu et al., 2000). Therefore, conversion of Arg, Pro, and Glu to N^6-acetylornithine (Figure 2B) would make nitrogen in phloem sap less available for aphids.

Observations of reduced *M. persicae* growth after MeJA treatment (Ellis et al., 2002) and improved growth on a *coi1* mutant relative to the wild type (Mewis et al., 2005) show that the JA signaling pathway contributes to aphid defense in *Arabidopsis*. However, although caterpillar herbivory strongly induces
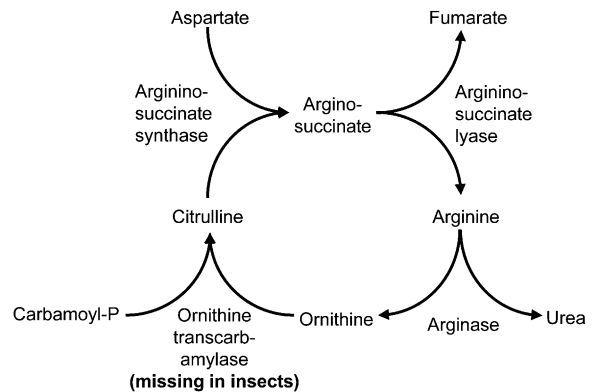

Figure 9. The Urea Cycle Allows Synthesis of Arg from Orn.

This metabolic cycle is incomplete in insects due to lack of Orn transcarbamylase, thereby preventing synthesis of Arg from Orn. Aphids lack all enzymes of the urea cycle but contain endosymbiont *Buchnera* bacteria that are capable of Arg biosynthesis from Orn.

JA-related genes, this is not the case for aphid feeding (Bidart-Bouzat and Kliebenstein, 2011). These differences in JA induction likely cause greater N^δ-acetylornithine accumulation in response to caterpillars (Figure 6B) than aphids (Figure 5D) and may represent active suppression of JA-regulated defenses by phloem-feeding insects (Zarate et al., 2007). ABA-regulated *NATA1* expression also causes elevated N^δ-acetylornithine accumulation (Figure 1D). Publicly available microarray data show overlapping gene expression patterns induced by aphid feeding and ABA (www.genevestigator.com; Zimmermann et al., 2004), and heavier aphid infestation of *Arabidopsis* induces wilting that could lead to ABA-regulated gene expression changes.

Several prior studies show that coronatine promotes *P. syringae* growth on *Arabidopsis* and tomato (Feys et al., 1994; Kloek et al., 2001; Zhao et al., 2003; Cui et al., 2005; Laurie-Berry et al., 2006; Uppalapati et al., 2007, 2008, 2011; Fernández-Calvo et al., 2011). Although induction of JA-regulated gene expression by coronatine likely suppresses SA-mediated plant defenses, other molecular mechanisms that connect COI1 to increased *P. syringae* growth remain unknown. Our observation of improved *P. syringae* growth in the *nata1-1* mutant background (Figure 4D) suggests that some of the observed NATA1-requiring metabolic changes (Figure 7) contribute to pathogen resistance. However, more direct effects on Orn-related metabolism also may be relevant for *P. syringae* virulence. WIN1 (At1g80600), a predicted N^α-acetylornithine transaminase, interacts directly with the *P. syringae* effector HopW1-1, and WIN1 overexpression prevents elicitation of *Arabidopsis* defenses by HopW1-1 and other *P. syringae* effectors (Lee et al., 2008).

In proceeding from the discovery of N^δ-acetylornithine, a previously unknown *Arabidopsis* metabolite, to the elucidation of a biosynthetic pathway and defense-related functions, we applied several of the excellent genetic and genomic resources that are available for *Arabidopsis*. Many recent studies of *Arabidopsis* defense mechanisms started with the identification of defense-related gene expression or mutants to identify new metabolites and signaling pathways. However, given the well-annotated *Arabidopsis* genome and extensive gene expression data sets, it now may be easier to move from identifying a novel plant metabolite to the discovery of a previously unknown enzymatic activity than vice versa. Our results, which have implications for research on both plant–pathogen and plant–herbivore interactions, provide new insight into the induction of biotic stress responses in plants.

METHODS

Plants and Growth Conditions

Seeds of *Arabidopsis thaliana* accessions (see Supplemental Table 1 online) and other Brassicaceae (see Supplemental Table 2 online) were obtained from the ABRC (www.Arabidopsis.org), T. Mitchell-Olds (Duke University, Durham, NC), and J. Jaworski (Danforth Center, St. Louis, MO). Seeds of other species were supplied by T. Brutnell (Boyce Thompson Institute, Ithaca, NY; *Zea mays*, *Brachypodium distachion*, and *Setaria viridis*), M. Kovach (Cornell University, Ithaca, NY; *Oryza sativa*), and N. Pumplin (Boyce Thompson Institute, Ithaca, NY; *Medicago truncatula*). Seeds of homozygous mutant *argah1-1* (SALK_057987; Alonso et al., 2003) and *argah2-1* (SAIL_181_C11; Sessions et al., 2002)

were from C. Todd (University of Saskatchewan, Saskatoon, Canada; Flores et al., 2008). Homozygous *fls2* mutant seeds were supplied by S. He (Michigan State University, East Lansing, MI; Zeng and He, 2010). *Arabidopsis coi1* (Feys et al., 1994), *npr1* (Cao et al., 1994), *sid1* (Nawrath et al., 2002), and *pad4* (Glazebrook et al., 1996) mutants were obtained from F. Ausubel (Massachusetts General Hospital, Boston, MA). The T-DNA insertion lines GK-256F07 (*nata1-1*; Rosso et al., 2003) and SALK_092319 (At2g39020 mutation; Alonso et al., 2003) were obtained from the ABRC. All plants were grown in Cornell mix (by weight 56% peat moss, 35% vermiculite, 4% lime, 4% Osmocoat slow-release fertilizer [Scotts], and 1% Unimix [Peters]) in 20 × 40-cm nursery flats in Conviron growth chambers with a photosynthetic photon flux density of 200 mmol $m^{-2} s^{-1}$ and a 16-h photoperiod at 23°C with a 50% relative humidity.

Isolation and Purification of N^δ-Acetylornithine

Five-week-old *Arabidopsis* plants were sprayed with 0.45 mM MeJA, and ~620 g leaves were harvested, frozen with liquid nitrogen, and homogenized in 1.5 liters of 80% methanol. The extract was concentrated by evaporation and partitioned with dichloromethane. The aqueous fraction was passed through DEAE-Sephadex A-25 column to extract the glucosinolate fraction for a separate experiment. The eluate from the Sephadex A-25 was then passed through a packed column of Dowex-50WX8-200 ion-exchange resin. The column was washed repeatedly with water, and amino acids were eluted with 200 mL 4 N NH₄OH followed by 100 mL water. Pooled eluate was lyophilized to leave 237 mg extract, which was then dissolved in 3 mL triethylamine (TEA) solution (2:2:1 of ethanol:water:TEA). The extract was then derivatized for 30 min in 1.26 mL phenylisothiocyanate (PITC) solution (980 μL ethanol, 70 μL water, 70 μL TEA, and 140 μL PITC). The reaction mixture was concentrated to dryness, taken up in 400 μL TEA solution, and concentrated to dryness again, leaving 680 mg residue. The extract was successively fractionated with Sephadex-LH-20 and RP18 packed columns and eluted with 95:5 water:methanol. The fraction containing the target compound, retention time = 29.90 min, was tracked by HPLC-DAD (Waters 2695 pump system and 996 diode array detector) using an RP18 column (Nova-Pak). HPLC Solvent A was 140 mm sodium acetate with 0.05% TEA (final pH adjusted to 6.33 with acetic acid). Solvent B was 60% acetonitrile. The gradient used was as follows: 0 to 10 min, 99% A; 10 to 35 min, linear gradient to 65% A; 35 to 40 min, 65% A; 40 to 42 min, linear gradient to 100% B; 42 to 44 min, 100% B. Further purification was achieved using a Lichrosphere column with water and acetonitrile as solvents to produce 1.1 mg of the target compound. For the HPLC runs (Lichrosphere column: 5 RP-18, ECAP 250, 4.6-mm inside diameter, 5-mm particle size) the mobile phases were A, water, and B, 90% acetonitrile, at a flow rate of 1.1 mL min^{-1} at 23°C. Column linear gradients for the samples were as follows: 0 to 1 min 75% A; 1 to 10 min, 60% A; 10 to 20 min 40% A; 20 to 30 min, 25% A; 30 to 35 min, 0% A; 35 to 40 min, 75% A.

The purified compound was analyzed by NMR. The (+ve)-ESI-MS spectrum showed an abundant molecular ion [M+PITC+Na]⁺ peak at 332, in addition to 175 [M+H-PITC]⁺ and 310 [M+H+PITC]⁺. In (−ve)-ESI-MS mode, the molecular ion was also detected with a peak [M+PITC-H]⁻ at mass-to-charge ratio (*m/z*) 308 in addition to 173 [M-H-PITC]⁻. Therefore, a molecular weight of 174 was assigned to the isolated compound. From the ¹HNMR, HMBC, and ESI-MS data, the isolated compound was assigned the structure of N^δ-acetylornithine. To further confirm the assigned structure, the isolated compound was compared with all possible acetylated products obtained after the treatment of L-Orn with glacial acetic acid and acetic acid anhydride after PITC derivatization. The isolated compound coeluted with N^δ-acetylornithine (retention time = 29.90 min.). Optical rotation measurements to determine whether *Arabidopsis* N^δ-acetylornithine has the L or D configuration were performed with a Polarimeter 241 (Perkin-Elmer) at 589 nm at 20°C using a sodium lamp.

Synthesis of N^6-Acetylornithine

N^6-Acetylornithine was synthesized from L-Orn and 4-nitrophenyl acetate (Leclerc and Benoiton, 1968). L-Orn monohydrochloride (0.5 g, 5.95 mmol) was dissolved in 5 mL water, and the pH was adjusted to 11 with 2 M NaOH. 4-Nitrophenyl acetate (1.07 g, 11.9 mmol) was then added and the mixture was stirred on ice. The mixture was stirred at room temperature for 4 h, concentrated to dryness with a Rotavap evaporator (Buchi), dissolved in 2 mL water, and partitioned repeatedly with ethyl acetate. The aqueous fraction containing the target compound was concentrated to dryness and redissolved in water followed by treatment with 0.1 M HCl to pH 4, until the mixture became colorless. Ethanol was added to the mixture and the precipitate was filtered with Buchner funnel to give a white precipitate (0.40 g). The precipitate was washed repeatedly with ethanol. The identity of synthesized N^6-acetylornithine was confirmed by 1D- and 2D-NMR and ESI-MS. The corresponding ESI-MS spectral data are as follows: ESI-MS (negative, m/z, relative abundance): $[M-H]^-$ (m/z); [173] (100).

GC-MS (Varian 1200L; Agilent Technologies) analysis of N-methyl-N-(trimethylsilyl)trifluoroacetamide + 1% trichloromethylsilane derivatized synthetic N^6-acetylornithine (retention time = 23.5 min [M+2TMS] and retention time = 23.95 min [M+1TMS]) was identical to the induced endogenous $Arabidopsis$ N^6-acetylornithine. Coelution of the synthetic and the naturally occurring compounds both on HPLC and GC further confirmed its identity. The ^{1}H-NMR spectral data of the synthesized N^6-acetylornithine were identical to those of earlier reports (Wohlfarth et al., 1993). The ^{1}H-NMR (D_2O) spectrum of N^6-acetylornithine established the following: ^{1}H-NMR (500 MHz, D_2O) δ: 3.59 (1H, t, J = 6 Hz), 3.09 to 3.02 (2H, m), 1.82 (3H, s), 1.76 to 1.66 (2H, m), 1.49 to 1.36 (2H, m).The ^{13}C-NMR extracted from the HMBC data revealed seven carbon atoms: 174.33, 174.08, 54.57, 38.63, 27.83, 24.26, and 22.02. GC-MS data of N^6-acetylornithine with 2-TMS derivatives gave an EI spectrum with m/z (%) 318 [1.7, M+2TMSi], 201 (22, M–CO_2TMSi), 112 (100, M-$C_2NH_4O_2$-2TMSi), 75(76), and 73(55).

Amino Acid Assays

For analysis of leaf amino acids, 100 mg of plant tissue was frozen in liquid nitrogen in 2-mL microcentrifuge tubes and ground to fine powder with 3-mm steel beads using a Harbil model 5G-HD paint shaker. Ground tissue was taken up in 20 mM HCl (10 μL/mg of tissue), the extracts were centrifuged at 3800g for 20 min at 23°C, and the supernatant was saved for analysis. Phloem sap was collected from rosettes of 3-week-old Col-0 plants sprayed with water or 0.45 mM MeJA treatment. Roots were cut from the rosettes, leaving 1 mm of the shoot tissue, and put in 100 μL of 15 mM EDTA solution, pH 7.7, for 4 h in the dark with high humidity. Fifteen samples were pooled for each replicate of the experiment. For analysis of N^6-acetylornithine uptake, $nata1-1$ leaf petioles were immersed in N^6-acetylornithine solutions in a 1.5-mL microcentrifuge tube for 24 h prior to tissue harvest. The petiole and other portions of the leaf that were immersed in the N^6-acetylornithine solution were not used for the amino acid analysis. For the measurement of N^6-acetylornithine in aphid bodies, aphids were collected from Col-0 plants treated with water or MeJA and transferred into a 2 mL centrifuge tube containing three 3-mm steel balls. The aphids were homogenized and extracted with 20 mM HCl. For aphid honeydew collection, ∼50 aphids were placed on artificial diet with and without N^6-acetylornithine for 4 d, and honeydew was collected on aluminum foil. The aluminum foil was washed with 80% methanol to extract amino acids. The methanolic extract was concentrated to dryness a SpeedVac rotary evaporator and then redissolved in 40 μL 20 mM HCl.

Amino acids were derivatized with 6-aminoquinolyl-N-hydroxysuccinimidylcarbamate using an AccQ-Fluor reagent kit (Waters). For derivatization, 5 μL extracts were mixed with 35 μL borate buffer and the reaction was initiated by the addition of 10 μL 6-aminoquinolyl-N-hydroxysucci-

nimidyl carbamate reagent, followed by immediate mixing and incubation for10 min at 55°C. Ten microliters of each sample were injected onto a Nova-Pak C18 column using a Waters 2695 pump system, and the data were recorded using Waters' Empower Software. L-Norleucine was used as an internal standard. Eluted amino acid derivatives were detected using a Waters model 2475 fluorescence detector with an excitation wavelength of 250 nm and an emission wavelength of 395 nm. Solvent A (containing sodium acetate and TEA at pH 5.05) was purchased premixed from Waters; Solvent B was acetonitrile:water (60:40). The gradient used was 0 to 0.01 min, 100% A; 0.01 to 0.5 min, linear gradient to 3% B; 0.5 to 12 min, linear gradient to 5% B; 12 to 15 min, linear gradient to 8% B; 15 to 45 min, 35% B; 45 to 49 min, linear gradient to 35% B; 50 to 60 min, 100% B. Flow rate was 1.0 mL min^{-1}.

Glucosinolate Assays

Leaves of 3-week old Col-0 wild-type $nata1-1$ $Arabidopsis$, with or without MeJA treatment, were collected and lyophilized. Extraction of plant tissue and preparation of desulphoglucosinolates was done as described previously (Kim et al., 2004; Barth and Jander, 2006). Desulphoglucosinolates were separated using a Waters 2695 HPLC and detected using a Waters 2996 photodiode array detector. For HPLC separation, the mobile phases were A, water, and B, 90% acetonitrile, with a flow rate of 1 mL/min at 23°C. Column linear gradients for samples were: 0 to 1 min, 98% A; 1 to 6 min 94% A; 6 to 8 min, 92% A; 8 to 16 min, 77% A; 16 to 20 min, 60% A; 20 to 25 min, 0% A; 25 to 27 min hold 0% A; 27 to 28 min, 98% A; 28 to 37 min, 98% A.

MeJA, SA, ACC, ABA, and Coronatine Induction

The leaves of 4-week-old $Arabidopsis$ plants were sprayed with aqueous solution containing 0.01% (v/v) Tween 20, supplemented with each of 0.45 mM SA, 0.45 mM MeJA, 0.45 mM ACC, and 0.1 mM ABA, a combination of both SA and MeJA, 1 μM coronatine, or 10 μM coronatine. Control plants were treated with 0.01% Tween 20 only. Controls for MeJA treatment also contained 0.03% acetone. Plants were covered and harvested 4 d after elicitation (or at multiple times for a time course of induction) and immediately frozen in liquid nitrogen. Pulverized plants were extracted with 20 mM HCl, and amino acids were analyzed as described above.

For time-course experiments, 2-week-old $Arabidopsis$ plants were treated with 0.45 mM MeJA, and leaves were harvested after 0 to 15 d. Leaves were frozen in liquid nitrogen and stored at −80°C before amino acid analysis as described above. For a separate experiment, the whole aerial parts were cut just above the root and weighed.

Stable Isotope Labeling Experiments

Petioles of a detached Col-0 leaves from 4-week-old plants were inserted into 1.5 mL microcentrifuge tubes containing 5 mM labeled amino acid ($[^{13}C_5]$Glu, $[^{13}C_6]$Arg, and $[^{13}C_5]$Pro) in water. In the case of Glu, 0.01% NaOH was used to aid solubility. Control leaves were treated with water only and allowed to stand for 12 h. After 12 h, leaves were sprayed with 0.45 mM MeJA. Leaf samples were covered and allowed to stand for 3 d. Three leaves receiving the same treatment were combined as one replicate for derivatization and GC-MS analysis of amino acids, as described above.

Amino acid analysis by GC-MS was performed as described previously (Joshi and Jander, 2009) with minor modifications. Single leaves harvested from $Arabidopsis$ Col-0 wild type and $nata1-1$ mutant at the same developmental stages were used. Leaves were frozen in liquid nitrogen in 2-mL tubes and ground to fine powder with 3-mm steel beads using a Harbil model 5G-HD paint shaker. Ground tissue was taken up in 20 mM HCl (1 mL per leaf tissue), the extracts were centrifuged at 4000g for 20 min at 23°C, and the supernatant leaf acid extracts were applied to Dowex-50 columns (0.6 mL). These were eluted individually with 6 M

NH_4OH (1 mL). Fractions were combined, and solutions were concentrated to 200 μL with a rotary evaporator. These extracts were then completely dried under nitrogen flow, with heating at 70°C. Methoxyamine hydrochloride in anhydrous pyridine (50 μL, 15 mg mL^{-1}) was added to the residue and the sample was heated at 30°C for 90 min. A volume of 90 μL N-methyl-N-(trimethylsilyl)trifluoroacetamide + 1% trimethylchlorosilane was then added, and the sample was heated for a further 30 min at 70°C. GC-MS analysis was performed using a Varian 1200L GC-MS with a DB-17 ms capillary column. Spectra of known amino acids were assigned by reference to an in-house spectral library and the NIST library.

Confirmation of T-DNA Insertions and Expression of Transgenes

Homozygous T-DNA insertions in *NATA1* (GK-256F07; Rosso et al., 2003) and At2g39020 (Salk_092319; Alonso et al., 2003) were confirmed by PCR using a previously outlined strategy using three primers to amplify both the insertion junction and the genomic DNA without an insertion (http://signal.salk.edu/tdnaprimers.2.html) and primers described in Supplemental Table 3 online. PCR reactions were run using Taq DNA polymerase (Fisher) under the following conditions: 95°C for 5 min, 40 cycles of 95°C for 1 min, 55°C for 1 min and 72°C for 1 min, followed by 72°C for 10 min.

For transgenic expression, *NATA1* and At2g39020 were cloned behind the cauliflower mosaic virus 35S promoter in the T-DNA binary vector pMDC32 (Curtis and Grossniklaus, 2003) using the Gateway recombination system (Invitrogen), and inserts were confirmed by DNA sequencing. Stable *Arabidopsis* p35S:*NATA1* transgenics were made by dipping transformation with *Agrobacterium tumefaciens* strain GV3101 (Clough and Bent, 1998). Seeds collected from transformed *Arabidopsis* plants were selected on agar containing 40 mg mL^{-1} hygromycin, and transgene expression was confirmed by qRT-PCR. The same T-DNA plasmids in GV3010 were used for transient expression of *NATA1* and At2g39020 in tobacco (*Nicotiana benthamiana* and *Nicotiana tabacum*) by *Agrobacterium* infiltration (Voinnet et al., 1998). *Agrobacterium* was cultured overnight at 30°C in Luria-Bertani (LB) broth supplemented with 50 μg mL^{-1} rifampicin, 25 μg mL^{-1} gentamycin, and 100 μg mL^{-1} kanamycin. Bacterial cultures were centrifuged at 8000g, washed three times with sterile water, and resuspended in sterile water to 0.2×10^8 colony-forming units/mL. Cultures were mixed with *Agrobacterium* (0.1×10^8/mL) carrying T-DNA constructs expressing the turnip crinkle virus capsid protein (P38; Thomas et al., 2003) to reduce expression silencing. *N. benthamiana* or *N. tabacum* leaves (four leaves per plant) were infiltrated with 1 mL bacterial solution using a 1 mL syringe. Excess bacterial solution was wiped off with paper towel. Three days after infiltration, leaf plugs (8-mm diameter) were collected to confirm expression of the transgenes by qRT-PCR.

qRT-PCR

Total RNA was extracted from frozen tissue samples using the SV Total RNA Isolation system with on-column DNase treatment (Promega). RNA integrity was verified using a 1.2% formaldehyde agarose gel (Sambrook et al., 1989). Transcript abundance of *NATA1* was analyzed with qRT-PCR, using *eEF1-α* (elongation factor 1-α, At5g60390) as an internal standard. *eEF1-α* was identified from publicly available microarray data as constitutively expressed before and after herbivory, and stable expression was verified across samples using qRT-PCR. After RNA extraction and DNase treatment, 1 μg of total RNA was reverse transcribed with SMART MMLV reverse transcriptase (Clonetech) using oligo-dT$_{12-18}$ as a primer. Gene-specific primers used for qRT-PCR were designed using Primer-Blast (http://www.ncbi.nlm.nih.gov/tools/primer-blast/) with the following criteria: temperature of 60°C, PCR amplicon lengths of 90 to 150

bp, primer sequences with lengths of 18 to 24 nucleotides with an optimum at 21 nucleotides, and GC contents of 40 to 60%. Primers for amplifying *NATA1* and *eEF1-α* are described in Supplemental Table 3 online. Reactions were performed using 5 μL of the SYBR Green PCR master mix (Applied Biosystems), with 800 nM of primer, in the 7900HT instrument (Applied Biosystems). The PCR was initiated by incubation at 95°C for 10 min to activate the enzyme. Then the following cycle was repeated 40 times: 95°C for 15 s, 60°C for 15 s, and 72°C for 15 s. The C_T values were quantified and analyzed according to the standard curve method.

GC-MS Metabolomics

For metabolomic analysis, 3-week-old wild-type and *nata1-1* mutant plants treated with water or 0.45 mM MeJA. After 4 d, 6.5-mm disks was taken from the central part of the first and second adult leaves of each plant. The two disks were combined and stored into a 2-mL microcentrifuge tubes put on ice. One milliliter of prechilled extraction buffer (acetonitrile:isopropanol:water [3:3:2]) and one metal ball were added to the sample. Plant tissue was macerated briefly for 30 s using a Harbil model 5G-HD paint shaker. Extracts were centrifuged at 4000g for 2 min at 4°C. Supernatants from each sample (400 μL) were transferred into new 2-mL tubes and stored at −80°C until automated derivatization and GC-TOF-MS analysis at the UC Davis Genome Center Metabolomics Facility (http://metabolomics-core.ucdavis.edu/; Fiehn et al., 2005). Metabolite identity was determined by comparing retention time and mass to the UC Davis Genome Center Metabolomics Facility metabolites database (http://fiehnlab.ucdavis.edu/Metabolite-Library-2007/; Fiehn et al., 2005). This library contains reference spectra for 713 known metabolites, generated by the analysis of purified reference compounds. Metabolites not contained within this library are listed as unknown or unidentified metabolites. After analysis, samples were subject to quality control by further analysis of samples with internal standard values >3 σ from the experimental mean within a given experiment, suggesting faulty derivatization or GC-TOF analysis of that specific sample.

Bacterial Bioassays

Pseudomonas syringae strains were supplied by H.G. Kang (Boyce Thompson Institute, Ithaca, NY; DC3000 *AvrRpt2* and DC3000 *AvrRpm1*), C. Danna (Massachusetts General Hospital, Boston, MA; Psm4326 and Psm4326 Cor-), and N. Clay (Yale University, New Haven, CT; PstDC3000 and PstDC3000 Cor-). For assays of N^δ-acetylornithine production in *Arabidopsis*, *P. syringae* was cultured at 30°C in LB broth. Bacteria were centrifuged and resuspended in water at an OD$_{600}$ of 0.2. Bacterial suspensions containing 0.01% Tween 20 were sprayed on *Arabidopsis* plants. Control plants are sprayed with water containing 0.01% Tween 20 only. After 4 d, infected leaves were collected for amino acid analysis as described above.

For in vitro growth experiments, *P. syringae* strain DC3000 was cultured at 30°C in modified mannitol-glutamate medium (Kean et al., 1970; per liter: 10 g mannitol, 2 g L^{-1} Glu, 0.5 g KH$_2$PO$_4$, 0.2 g NaCl, 0.2 g MgSO$_4$-7H$_2$O; pH adjusted to 7.0 with 3 N NaOH prior to autoclaving). To test growth with other amino acids as nitrogen sources, Glu was replaced successively with 2 g L^{-1} Arg, Pro, Orn, N^α-acetylornithine, and N^δ-acetylornithine. Cultures were inoculated by diluting a fresh overnight culture of *P. syringae* 1:100 (50 μL into 5 mL). OD$_{600}$ was measured at 0, 14, 48, and 72 h after treatment. For growth inhibition experiments, cultures were grown in minimal medium with 2 g L^{-1} Glu and 0, 10, 100, 250, or 500 μM N^δ-acetylornithine.

For in planta growth experiments, *P. syringae* PstDC3000 was cultured at 30°C in LB broth supplemented with 50 μg mL^{-1} rifampicin, centrifuged, resuspended in sterile water, and diluted to a concentration of 10^5 colony-forming units/mL. Col-0 wild-type and *nata1-1* leaves were

infiltrated with 0.2 mL bacterial solution using a 1-mL syringe. Excess bacterial solution was wiped off with paper towel. Leaf plugs (8-mm diameter) were collected at 0, 2, and 4 d after infiltration. Leaf discs were floated in 1 mL sterile water with 0.01% Tween 20 on a shaker for ~2 h. Ten-microliter samples of a bacterial dilution series were spotted on an LB agar plate containing 50 μg mL^{-1} rifampicin and incubated at 30°C. Bacterial colonies were counted after 2 d, and the concentration of bacteria in the leaf plugs was calculated.

Caterpillar Bioassays

The *Pieris rapae* were from a colony maintained by the Jander laboratory, which is descended from 20 adult insects collected in the wild on the Cornell University campus in July, 2008. *Plutella xylostella* eggs were obtained from Benzon Research. Neonate caterpillars were confined on the leaves of 3-week-old wild-type and *nata1-1* plants using mesh-covered cups. *P. rapae* were allowed to feed on plants for 7 d before harvesting. *P. xylostella* were harvested after pupation. Caterpillars and pupae were lyophilized and dry weight was determined using a precision balance (Sartorius). Mutant and wild-type leaves infested by caterpillar were also collected for amino acid analysis as described above.

Aphid Bioassays

Artificial diet for *Myzus persicae* fecundity assays consisted of Suc (440 mM) and 20 amino acids (Ala, 10 mM; Arg, 16 mM; Asn, 20 mM; Asp, 10 mM; Cys, 3.3 mM; Glu, 10 mM; Gln, 10 mM; Gly, 10 mM; His, 10 mM; Ile, 6 mM; Leu, 6 mM; Lys, 10 mM; Met, 5 mM; Phe, 3 mM; Pro, 7 mM; Ser, 10 mM; Thr, 12 mM; Trp, 4 mM; Tyr, 2 mM; Val, 7 mM). Zero, 0.1, 0.5, 5, or 10 mM N^{δ}-acetylornithine was added to the diet. For experiments with a single amino acid as the nitrogen source, Orn, Glu, and N^{δ}-acetylornithine were added at 10 mM concentration to 440 mM Suc. One wingless adult aphid was placed in a 30-mL plastic cup that was covered with a Parafilm sachet containing 100 μL of the liquid diet. Aphid nymphs were counted after 4 d.

M. persicae reproduction was compared on *Arabidopsis* Col-0 wild type and *nata1-1*, with and without MeJA treatment. Plants were covered after MeJA application for 48 h. The cover was then removed 48 h prior to the caging aphids on *Arabidopsis* flower stalks or rosette leaves. Plant trays with and without MeJA were separated and covered to prevent volatiles induced by MeJA from eliciting defenses in control plants. Aphid progeny production was recorded after 7 d. For *N. tabacum* experiments, aphids were caged on individual leaves in the area where *Agrobacterium* constructs had been infiltrated 3 d previously, and progeny production was assessed 7 d later.

To assess effects of exogenously added N^{δ}-acetylornithine, petioles from mature leaves of 4-week-old *nata1-1* plants were inserted in 1.5-mL microcentrifuge tubes containing 0, 0.1, or 0.5 mM N^{δ}-acetylornithine in water. After 24 h, one aphid was placed on each individual leaf, and aphid progeny production was recorded after 4 d.

Sequence Alignment and Phylogenetic Tree Generation

Arabidopsis NATA1 homologs in the Brassicaceae (*Arabidopsis lyrata*, *Brassica rapa*, *Brassica napus, Raphanus raphanistrum*, and *Capsella rubella*) were obtained by comparison to genomic and EST data in GenBank. The closest *NATA1* homolog of *Carica papaya* in the Caricaceae, a related family in the Brassicales, was used as an outgroup. Multiple sequence alignment of translated protein sequences was performed with ClustalW (Larkin et al., 2007). Programs in the PHYLIP version 3.6 software package (Felsenstein, 2005) were used to create a phylogenetic tree. The SEQBOOT function was used to make 1000 bootstrapped data sets. PROMLK was used to construct rooted phylogenetic trees, using the parameters search for the best tree, Jones-Taylor-Thornton probability model, one category of substitution rates, constant rate variation among

sites, no global rearrangement, no weighted sites, and randomization of input sequences. A rooted consensus tree was made with CONSENSE using the majority rule (extended) parameter.

Accession Numbers

Supplemental Data

The following materials are available in the online version of this article.

   Supplemental Figure 1. Identification of N^{δ}-Acetylornithine by MS and NMR.

   Supplemental Figure 2. N^{δ}-Acetylornithine Is Distinct from the Common Plant Metabolite N^{α}-Acetylornithine.

   Supplemental Figure 3. N^{δ}-Acetylornithine Accumulation in *Arabidopsis* Foliage after Elicitation with Abscisic Acid.

   Supplemental Figure 4. Pathways for Incorporation of [U-^{13}C]Arg, [U-^{13}C]Pro, and [U-^{13}C]Glu into N^{δ}-Acetylornithine.

   Supplemental Figure 5. Accumulation of Free Amino Acids in Foliage of *nata-1* Mutant and *nata1-1* p35S:*NATA1* Plants.

   Supplemental Figure 6. N^{δ}-Acetylornithine Accumulation in *fls2* Mutant *Arabidopsis* after *P. syringae* Treatment.

   Supplemental Figure 7. Abundance of Transport Amino Acids in Phloem Exudates after MeJA Treatment.

   Supplemental Figure 8. Free Amino Acids in *nata1-1* Mutant Leaves with and without Added N^{δ}-Acetylornithine.

   Supplemental Figure 9. Aphid Reproduction on an Artificial Diet with a Single Amino Acid as the Nitrogen Source.

   Supplemental Figure 10. Glucosinolate Accumulation in Col-0 and *nata1-1*, with and without MeJA Treatment.

   Supplemental Figure 11. Polyamine Accumulation in Col-0 and *nata1-1*, with and without MeJA Treatment.

   Supplemental Figure 12. Free Amino Acids in Control and MeJA-Induced Col-0 Wild Type and *nata1-1* Mutants.

   Supplemental Figure 13. Growth of Col-0 Wild Type and *nata1-1*, with and without MeJA Treatment.

   Supplemental Table 1. *Arabidopsis* Isolates That Show MeJA-Induced Production of N^{δ}-Acetylornithine.

   Supplemental Table 2. Crucifers That Were Tested for the Presence of N^{δ}-Acetylornithine.

   Supplemental Table 3. PCR Primers Used in This Study.

   Supplemental Data Set 1. Metabolite Profiling of Col-0 Wild-Type and *nata1-1* Mutant Leaves, with and without MeJA Treatment.

Supplemental Data Set 2. ClustalW Sequence Alignment of NATA1 Homologs in the Brassicaceae.

AUTHOR CONTRIBUTIONS

A.M.A. and G.J. designed the research. A.M.A., C.L.S., M.D.V., J.H.K., V.J., B.L., C.J., J.D., and G.J. performed research. A.M.A., C.L.C., M.D.V., J.H.K., V.J., D.J.K., and G.J. analyzed data. A.M.A. and G.J. wrote the article.

REFERENCES

Adams, M.D., et al. (2000). The genome sequence of *Drosophila melanogaster*. Science **287:** 2185–2195.

Agrawal, A.A. (1998). Induced responses to herbivory and increased plant performance. Science **279:** 1201–1202.

Agrawal, A.A. (2000). Overcompensation of plants in response to herbivory and the by-product benefits of mutualism. Trends Plant Sci. **5:** 309–313.

Alonso, J.M., et al. (2003). Genome-wide insertional mutagenesis of *Arabidopsis thaliana*. Science **301:** 653–657.

Barth, C., and Jander, G. (2006). Arabidopsis myrosinases TGG1 and TGG2 have redundant function in glucosinolate breakdown and insect defense. Plant J. **46:** 549–562.

Bednarek, P., Schneider, B., Svatos, A., Oldham, N.J., and Hahlbrock, K. (2005). Structural complexity, differential response to infection, and tissue specificity of indolic and phenylpropanoid secondary metabolism in Arabidopsis roots. Plant Physiol. **138:** 1058–1070.

Bell, E.A. (2003). Nonprotein amino acids of plants: significance in medicine, nutrition, and agriculture. J. Agric. Food Chem. **51:** 2854–2865.

Bidart-Bouzat, M.G., and Kliebenstein, D. (May 31, 2011). An ecological genomic approach challenging the paradigm of differential plant responses to specialist versus generalist insect herbivores. Oecologia http://dx.doi.org/10.1007/s00442-011-2015-z.

Bino, R.J., et al. (2004). Potential of metabolomics as a functional genomics tool. Trends Plant Sci. **9:** 418–425.

Brooks, D.M., Hernández-Guzmán, G., Kloek, A.P., Alarcón-Chaidez, F., Sreedharan, A., Rangaswamy, V., Peñaloza-Vázquez, A., Bender, C.L., and Kunkel, B.N. (2004). Identification and characterization of a well-defined series of coronatine biosynthetic mutants of *Pseudomonas syringae* pv. *tomato* DC3000. Mol. Plant Microbe Interact. **17:** 162–174.

Brown, D.H., and Fowden, L. (1966). Characterization of δ-acetyl-*L*-ornithine isolated from *Onobrychis vicifolia* Scop. Phytochemistry **5:** 881–886.

Brownfield, D.L., Todd, C.D., and Deyholos, M.K. (2008). Analysis of Arabidopsis arginase gene transcription patterns indicates specific biological functions for recently diverged paralogs. Plant Mol. Biol. **67:** 429–440.

Cao, H., Bowling, S.A., Gordon, A.S., and Dong, X. (1994). Characterization of an *Arabidopsis* mutant that Is nonresponsive to inducers of systemic acquired resistance. Plant Cell **6:** 1583–1592.

Century, K.S., Holub, E.B., and Staskawicz, B.J. (1995). *NDR1*, a locus of *Arabidopsis thaliana* that is required for disease resistance to both a bacterial and a fungal pathogen. Proc. Natl. Acad. Sci. USA **92:** 6597–6601.

Chen, H., Wilkerson, C.G., Kuchar, J.A., Phinney, B.S., and Howe, G.A. (2005). Jasmonate-inducible plant enzymes degrade essential amino acids in the herbivore midgut. Proc. Natl. Acad. Sci. USA **102:** 19237–19242.

Chini, A., Fonseca, S., Fernández, G., Adie, B., Chico, J.M., Lorenzo, O., García-Casado, G., López-Vidriero, I., Lozano, F.M., Ponce, M.R., Micol, J.L., and Solano, R. (2007). The JAZ family of repressors is the missing link in jasmonate signalling. Nature **448:** 666–671.

Clay, N.K., Adio, A.M., Denoux, C., Jander, G., and Ausubel, F.M. (2009). Glucosinolate metabolites required for an Arabidopsis innate immune response. Science **323:** 95–101.

Clough, S.J., and Bent, A.F. (1998). Floral dip: a simplified method for *Agrobacterium*-mediated transformation of *Arabidopsis thaliana*. Plant J. **16:** 735–743.

Cui, J., Bahrami, A.K., Pringle, E.G., Hernandez-Guzman, G., Bender, C.L., Pierce, N.E., and Ausubel, F.M. (2005). *Pseudomonas syringae* manipulates systemic plant defenses against pathogens and herbivores. Proc. Natl. Acad. Sci. USA **102:** 1791–1796.

Curtis, M.D., and Grossniklaus, U. (2003). A gateway cloning vector set for high-throughput functional analysis of genes in planta. Plant Physiol. **133:** 462–469.

D'Auria, J.C., and Gershenzon, J. (2005). The secondary metabolism of *Arabidopsis thaliana*: Growing like a weed. Curr. Opin. Plant Biol. **8:** 308–316.

De Vos, M., and Jander, G. (2009). *Myzus persicae* (green peach aphid) salivary components induce defence responses in *Arabidopsis thaliana*. Plant Cell Environ. **32:** 1548–1560.

Dixon, R.A. (2001). Natural products and plant disease resistance. Nature **411:** 843–847.

Ellis, C., Karafyllidis, I., and Turner, J.G. (2002). Constitutive activation of jasmonate signaling in an Arabidopsis mutant correlates with enhanced resistance to *Erysiphe cichoracearum*, *Pseudomonas syringae*, and *Myzus persicae*. Mol. Plant Microbe Interact. **15:** 1025–1030.

Fan, J., Crooks, C., Creissen, G., Hill, L., Fairhurst, S., Doerner, P., and Lamb, C. (2011). *Pseudomonas sax* genes overcome aliphatic isothiocyanate-mediated non-host resistance in *Arabidopsis*. Science **331:** 1185–1188.

Felsenstein, J. (2005). PHYLIP (Phylogeny Inference Package) Version 3.6. (Seattle, WA: University of Washington).

Fernández-Calvo, P., et al. (2011). The *Arabidopsis* bHLH transcription factors MYC3 and MYC4 are targets of JAZ repressors and act additively with MYC2 in the activation of jasmonate responses. Plant Cell **23:** 701–715.

Feys, B., Benedetti, C.E., Penfold, C.N., and Turner, J.G. (1994). *Arabidopsis* mutants selected for resistance to the phytotoxin coronatine are male sterile, insensitive to methyl jasmonate, and resistant to a bacterial pathogen. Plant Cell **6:** 751–759.

Fiehn, O., Wohlgemuth, G., and Scholz, M. (2005). Setup and annotation of metabolomics experiments by integrating biological and mass spectrometric metadata. Lect. Not. Comp. Sci. **3615:** 224–239.

Flores, T., Todd, C.D., Tovar-Mendez, A., Dhanoa, P.K., Correa-Aragunde, N., Hoyos, M.E., Brownfield, D.M., Mullen, R.T., Lamattina,

L., and Polacco, J.C. (2008). Arginase-negative mutants of Arabidopsis exhibit increased nitric oxide signaling in root development. Plant Physiol. **147:** 1936–1946.

Fowden, L. (1958). δ-Acetylornithine: A constituent of some common grasses. Nature **182:** 406–407.

Fowden, L. (2001). Plant amino acid research in retrospect: From Chinball to Singh. Amino Acids **20:** 217–224.

Glazebrook, J., Rogers, E.E., and Ausubel, F.M. (1996). Isolation of Arabidopsis mutants with enhanced disease susceptibility by direct screening. Genetics **143:** 973–982.

Halkier, B.A., and Gershenzon, J. (2006). Biology and biochemistry of glucosinolates. Annu. Rev. Plant Biol. **57:** 303–333.

Honeybee Genome Sequencing Consortium (2006). Insights into social insects from the genome of the honeybee *Apis mellifera*. Nature **443:** 931–949.

Howe, G.A., and Jander, G. (2008). Plant immunity to insect herbivores. Annu. Rev. Plant Biol. **59:** 41–66.

Joshi, V., and Jander, G. (2009). Arabidopsis methionine gamma-lyase is regulated according to isoleucine biosynthesis needs but plays a subordinate role to threonine deaminase. Plant Physiol. **151:** 367–378.

Kean, P.J., Kerr, A., and New, P.B. (1970). Crown gall of stone fruit: II, Identification and nomenclature of *Agrobacterium* isolates. Aust. J. Biol. Sci. **23:** 585–595.

Kessler, A., and Baldwin, I.T. (2002). Plant responses to insect herbivory: The emerging molecular analysis. Annu. Rev. Plant Biol. **53:** 299–328.

Kim, J.H., Durrett, T.P., Last, R.L., and Jander, G. (2004). Characterization of the Arabidopsis TU8 glucosinolate mutation, an allele of *TERMINAL FLOWER2*. Plant Mol. Biol. **54:** 671–682.

Kim, J.H., and Jander, G. (2007). *Myzus persicae* (green peach aphid) feeding on Arabidopsis induces the formation of a deterrent indole glucosinolate. Plant J. **49:** 1008–1019.

Kite, G.C., and Ireland, H. (2002). Non-protein amino acids of Bocoa (Leguminosae; Papilionoideae). Phytochemistry **59:** 163–168.

Kloek, A.P., Verbsky, M.L., Sharma, S.B., Schoelz, J.E., Vogel, J., Klessig, D.F., and Kunkel, B.N. (2001). Resistance to *Pseudomonas syringae* conferred by an *Arabidopsis thaliana* coronatine-insensitive (*coi1*) mutation occurs through two distinct mechanisms. Plant J. **26:** 509–522.

Lam, H.M., Wong, P., Chan, H.K., Yam, K.M., Chen, L., Chow, C.M., and Coruzzi, G.M. (2003). Overexpression of the *ASN1* gene enhances nitrogen status in seeds of Arabidopsis. Plant Physiol. **132:** 926–935.

Larkin, M.A., et al. (2007). Clustal W and Clustal X version 2.0. Bioinformatics **23:** 2947–2948.

Laurie-Berry, N., Joardar, V., Street, I.H., and Kunkel, B.N. (2006). The *Arabidopsis thaliana JASMONATE INSENSITIVE 1* gene is required for suppression of salicylic acid-dependent defenses during infection by *Pseudomonas syringae*. Mol. Plant Microbe Interact. **19:** 789–800.

Leclerc, J., and Benoiton, L. (1968). On the selectivity of acylation of unprotected diamino acids. Can. J. Chem. **46:** 1047–1051.

Lee, M.W., Jelenska, J., and Greenberg, J.T. (2008). Arabidopsis proteins important for modulating defense responses to *Pseudomonas syringae* that secrete HopW1-1. Plant J. **54:** 452–465.

Lemaître, T., Gaufichon, L., Boutet-Mercey, S., Christ, A., and Masclaux-Daubresse, C. (2008). Enzymatic and metabolic diagnostic of nitrogen deficiency in *Arabidopsis thaliana* Wassileskija accession. Plant Cell Physiol. **49:** 1056–1065.

Lipson, D.L., Raab, T.K., and Monson, R.K. (1996). δ-Acetylornithine as a major nitrogen storage compound in *Bistorta bistortoides*. Phytochemistry **41:** 29–30.

Manske, R.H.F. (1937). The natural occurence of acetyl-ornithine. Can. J. Res. **15B:** 84–87.

Marona, H.R.N., Schenkel, E.P., and Bergonoci, J.I. (2003). Phytotoxic activity of *Ateleia glazioviana* Baill. extracts on lettuce seeds. Acta Farm. Bonaerense **22:** 17–20.

Melotto, M., Underwood, W., Koczan, J., Nomura, K., and He, S.Y. (2006). Plant stomata function in innate immunity against bacterial invasion. Cell **126:** 969–980.

Mewis, I., Appel, H.M., Hom, A., Raina, R., and Schultz, J.C. (2005). Major signaling pathways modulate Arabidopsis glucosinolate accumulation and response to both phloem-feeding and chewing insects. Plant Physiol. **138:** 1149–1162.

Mur, L.A., Kenton, P., Atzorn, R., Miersch, O., and Wasternack, C. (2006). The outcomes of concentration-specific interactions between salicylate and jasmonate signaling include synergy, antagonism, and oxidative stress leading to cell death. Plant Physiol. **140:** 249–262.

Nawrath, C., Heck, S., Parinthawong, N., and Métraux, J.P. (2002). EDS5, an essential component of salicylic acid-dependent signaling for disease resistance in *Arabidopsis*, is a member of the MATE transporter family. Plant Cell **14:** 275–286.

Norris, R.D., and Fowden, L. (1972). Substrate discrimination by prolyl-*t*RNA synthetase from various higher plants. Phytochemistry **11:** 2921–2935.

Peterson, P.J., and Fowden, L. (1963). Different specificities of proline-activating enzymes from some plant species. Nature **200:** 148–151.

Pfalz, M., Vogel, H., and Kroymann, J. (2009). The gene controlling the indole glucosinolate modifier1 quantitative trait locus alters indole glucosinolate structures and aphid resistance in *Arabidopsis*. Plant Cell **21:** 985–999.

Reddy, S.R., and Campbell, J.W. (1977). Enzymic basis for the nutritional requirement of arginine in insects. Experientia **33:** 160–161.

Richards, S., et al.; Tribolium Genome Sequencing Consortium (2008). The genome of the model beetle and pest *Tribolium castaneum*. Nature **452:** 949–955.

Rosenthal, G.A. (2001). *L*-Canavanine: A higher plant insecticidal allelochemical. Amino Acids **21:** 319–330.

Rosso, M.G., Li, Y., Strizhov, N., Reiss, B., Dekker, K., and Weisshaar, B. (2003). An *Arabidopsis thaliana* T-DNA mutagenized population (GABI-Kat) for flanking sequence tag-based reverse genetics. Plant Mol. Biol. **53:** 247–259.

Sambrook, J., Fritsch, E.F., and Maniatis, T. (1989). Molecular Cloning: A Laboratory Manual, 2nd ed. (Cold Spring Harbor, NY: Cold Spring Harbor Laboratory Press).

Sessions, A., et al. (2002). A high-throughput *Arabidopsis* reverse genetics system. Plant Cell **14:** 2985–2994.

Shigenobu, S., Watanabe, H., Hattori, M., Sakaki, Y., and Ishikawa, H. (2000). Genome sequence of the endocellular bacterial symbiont of aphids *Buchnera* sp. APS. Nature **407:** 81–86.

Spoel, S.H., et al. (2003). NPR1 modulates cross-talk between salicylate- and jasmonate-dependent defense pathways through a novel function in the cytosol. Plant Cell **15:** 760–770.

Stowe, K.A., Marquis, R.J., Hochwender, C.G., and Simms, E.L. (2000). The evolutionary ecology of tolerance to consumer damage. Annu. Rev. Ecol. Syst. **31:** 565–595.

Thaler, J.S., Karban, R., Ullman, D.E., Boege, K., and Bostock, R.M. (2002). Cross-talk between jasmonate and salicylate plant defense pathways: Effects on several plant parasites. Oecologia **131:** 227–235.

Thines, B., Katsir, L., Melotto, M., Niu, Y., Mandaokar, A., Liu, G., Nomura, K., He, S.Y., Howe, G.A., and Browse, J. (2007). JAZ repressor proteins are targets of the SCF(COI1) complex during jasmonate signalling. Nature **448:** 661–665.

Thomas, C.L., Leh, V., Lederer, C., and Maule, A.J. (2003). Turnip crinkle virus coat protein mediates suppression of RNA silencing in *Nicotiana benthamiana*. Virology **306:** 33–41.

Tiffin, P. (2000). Mechanisms of tolerance to herbivore damage: What do we know? Evol. Ecol. **14:** 523–536.

Uppalapati, S.R., Ishiga, Y., Ryu, C.M., Ishiga, T., Wang, K., Noël, L.D., Parker, J.E., and Mysore, K.S. (2011). *SGT1* contributes to coronatine signaling and *Pseudomonas syringae* pv. *tomato* disease symptom development in tomato and Arabidopsis. New Phytol. **189:** 83–93.

Uppalapati, S.R., Ishiga, Y., Wangdi, T., Kunkel, B.N., Anand, A., Mysore, K.S., and Bender, C.L. (2007). The phytotoxin coronatine contributes to pathogen fitness and is required for suppression of salicylic acid accumulation in tomato inoculated with *Pseudomonas syringae* pv. *tomato* DC3000. Mol. Plant Microbe Interact. **20:** 955–965.

Uppalapati, S.R., Ishiga, Y., Wangdi, T., Urbanczyk-Wochniak, E., Ishiga, T., Mysore, K.S., and Bender, C.L. (2008). Pathogenicity of *Pseudomonas syringae* pv. *tomato* on tomato seedlings: phenotypic and gene expression analyses of the virulence function of coronatine. Mol. Plant Microbe Interact. **21:** 383–395.

Verslues, P.E., and Sharma, S. (2010). Proline metabolism and its implications for plant-environment interaction. In The Arabidopsis Book **8:** e0140, doi/10.1199/tab.0140.

Vetting, M.W., de Carvalho, L.P., Roderick, S.L., and Blanchard, J.S. (2005). A novel dimeric structure of the RimL Nalpha-acetyltransferase from *Salmonella typhimurium*. J. Biol. Chem. **280:** 22108–22114.

Virtanen, A.I., and Linko, P. (1955). The occurrence of free ornithine and it N-acetyl derivative in plants. Acta Chem. Scand. **9:** 531–554.

Voinnet, O., Vain, P., Angell, S., and Baulcombe, D.C. (1998). Systemic spread of sequence-specific transgene RNA degradation in plants is initiated by localized introduction of ectopic promoterless DNA. Cell **95:** 177–187.

Wenzel, C.L., Hester, Q., and Mattsson, J. (2008). Identification of genes expressed in vascular tissues using NPA-induced vascular overgrowth in Arabidopsis. Plant Cell Physiol. **49:** 457–468.

Whalen, M.C., Innes, R.W., Bent, A.F., and Staskawicz, B.J. (1991). Identification of *Pseudomonas syringae* pathogens of *Arabidopsis* and a bacterial locus determining avirulence on both *Arabidopsis* and soybean. Plant Cell **3:** 49–59.

Wilson, A.C., Ashton, P.D., Calevro, F., Charles, H., Colella, S., Febvay, G., Jander, G., Kushlan, P.F., Macdonald, S.J., Schwartz, J.F., Thomas, G.H., and Douglas, A.E. (2010). Genomic insight into the amino acid relations of the pea aphid, *Acyrthosiphon pisum*, with its symbiotic bacterium *Buchnera aphidicola*. Insect Mol. Biol. **19** (Suppl. 2): 249–258.

Wohlfarth, A., Severin, J., and Galinski, E.A. (1993). Identification of N-delta-acetylornithine as a novel osmolyte in some gram-positive halophilic eubacteria. Appl. Microbiol. Biotechnol. **39:** 568–573.

Yan, Y., Stolz, S., Chételat, A., Reymond, P., Pagni, M., Dubugnon, L., and Farmer, E.E. (2007). A downstream mediator in the growth repression limb of the jasmonate pathway. Plant Cell **19:** 2470–2483.

Zacharius, R.M. (1970). Composition of the nitrogenous components of the bush bean seed (*Phaseolus vulgaris*) including isolation of δ-*N*-acetylornithine. Phytochemistry **9:** 2047–2051.

Zarate, S.I., Kempema, L.A., and Walling, L.L. (2007). Silverleaf whitefly induces salicylic acid defenses and suppresses effectual jasmonic acid defenses. Plant Physiol. **143:** 866–875.

Zeng, W., and He, S.Y. (2010). A prominent role of the flagellin receptor FLAGELLIN-SENSING2 in mediating stomatal response to *Pseudomonas syringae* pv *tomato* DC3000 in Arabidopsis. Plant Physiol. **153:** 1188–1198.

Zhao, Y., Thilmony, R., Bender, C.L., Schaller, A., He, S.Y., and Howe, G.A. (2003). Virulence systems of *Pseudomonas syringae* pv. *tomato* promote bacterial speck disease in tomato by targeting the jasmonate signaling pathway. Plant J. **36:** 485–499.

Zhu, X., Shaw, P.N., Pritchard, J., Newbury, J., Hunt, E.J., and Barrett, D.A. (2005). Amino acid analysis by micellar electrokinetic chromatography with laser-induced fluorescence detection: application to nanolitre-volume biological samples from *Arabidopsis thaliana* and *Myzus persicae*. Electrophoresis **26:** 911–919.

Zimmermann, P., Hirsch-Hoffmann, M., Hennig, L., and Gruissem, W. (2004). GENEVESTIGATOR. Arabidopsis microarray database and analysis toolbox. Plant Physiol. **136:** 2621–2632.